AIChE WILEY InterScience DISCOVER SOMETHING GREAT

BIOENGINEERING, FOOD, AND NATURAL PRODUCTS

Effect of Dynamic Loading on Solute Transport in Soft Gels Implication for Drug Delivery

F. Urciuolo, G. Imparato, and P. A. Netti

Institute of Composite and Biomedical Materials (IMCB), National Council Research (CNR), P.Le Tecchio 80, 80125 Naples, Italy; Interdisciplinary Research Centre on Biomaterials (CRIB), University of Naples Federico II, P.le Tecchio 80, 80125 Naples, Italy; Dept. of Material Engineering and Production (DIMP), University of Naples Federico II, P.le Tecchio 80, 80125 Naples, Italy; Italian Institute of Technology (IIT), Via Morego 30, 16163 Genoa, Italy

DOI 10.1002/aic.11394

Published online January 8, 2008 in Wiley InterScience (www.interscience.wiley.com).

Solute transport through soft gels and tissues is intimately coupled to mechanical stress and deformation of the macromolecular network. The aim of this study was to investigate the effect of periodic mechanical stimuli upon solute transport through agarose gels at different concentrations. For this purpose it was experimentally evaluated the materials parameters that govern the coupling between elasto-dynamic and solute transport: hydraulic conductivity (K), elastic modulus (H_A), and macromolecular diffusivity (D_g) along with their strain dependence behavior. Mechanical activated solute transport simulation was carried out in order to elucidate the role of amplitude and frequency of soliciting mechanical stimuli on mass kinetics release. Results show that mechanical loading affects the release of macromolecules from a gel in a frequency and strain dependent manner. These findings pave the way for novel strategies for the design and engineering of smart drug delivery devices with transport mechanisms triggered by mechanical stimuli. © 2008 American Institute of Chemical Engineers *AIChE J,* 54: 824–834, 2008

Keywords: drug release, solute transport, FRAP, gel mechanics, agarose

Introduction

In the design of drug delivery systems for medicinal and biotechnological applications quite often the solute transport mechanisms through polymeric gels have been explored; for this purpose passive diffusion kinetic models[1–3] have been applied. In the mean time, it was soon established, that, other transport mechanisms could govern solute temporal and spatial delivery when the gel is under mechanical stress.[4–9] The role of external stimulation on solute transport has been extensively investigated in both polymeric gels and biological systems. While static compression has been shown to reduce solute diffusivity and partitioning in biphasic systems,[4] external stimulation that ultimately invoked fluid convection within the system could also induce an accelerated release kinetic.[5–7] The design of delivery systems and load history able to modulate and optimize macromolecular transport within such systems remains a major scientific and technological challenge.

Early works reported results obtained for polyelectrolyte systems that demonstrated the rise of solute transport rates when fluid movement was increased by electro-osmotic flow.[5] Fluid flow in soft gels can also result from applying a dynamic compression. Under these conditions, during studies performed on articular cartilage explants, it was witnessed enhanced tissue biosynthetic activity, whilst cyclical loading was found to induce protein transport, such as BSA and glucose-like solutes.[6–8] Furthermore, it has been possible to define an optimal combination of frequency and loading amplitude. In other applications, it has been established that dynamic mechanical environments regulate the release of VEGF encapsulated in polymeric

Correspondence concerning this article should be addressed to P. A. Netti at nettipa@unina.it.

gels; in this case, blood vessel formation was found to increase at the frequency and amplitude where growth factor release was accelerated.[9]

In the light of these findings, the successful engineering of drug delivery systems for several applications soon transformed into a short-term scientific and technological expectation. Towards that end, several mathematical models have been proposed. The multiphasic model is the most frequently applied to couple transport and mechanics in soft gels and tissue.[10–19] This approach, in particular, was used in the study of macromolecules transport in solid tumors subjected to constant pressure drug infusion.[13] Furthermore, in a similar study by taking into account the viscoelasticity of the solid fraction, transient solute evolution was shown to be affected by the relaxation time of the network.[14] Solute release under periodic mechanical loading was recently the subject of theoretical research.[15,16] The existence of an optimal combination of stimulation with material parameters that are able to enhance solute transport was also assessed.

In the present study, agarose gels at different concentrations have been used as models to survey macromolecular release under cyclical loading in the finite deformations range. The analysis presented herein consists of two-step process: firstly the experimental evaluation of key parameters, hydraulic conductivity (K), elastic modulus (H_A), and molecular diffusivity ratio (R) as a function of both gel composition and deformation has been carried out. The strain dependent hydraulic conductivity relationship and elastic modulus for agarose gels at different concentrations has been assessed by means of incremental stress relaxation test.[17–19] FRAP technique[19,20] has been employed to evaluate effective molecular diffusivity of BSA 67KDa in the gels (D_g) and in free solution (D_0). Therefore, values of diffusivity ratio R ($= D_g/D_0$) has been obtained. In order to obtain a molecular diffusivity coefficient sensitive to deformation,[21,22] Brinkmans' equation has been coupled with the hydraulic conductivity vs. strain relationship.

In the second step, experimental data have been used as input material parameters to perform simulations on solute transport in agarose gels subjected to periodic compressive stimuli.

Mathematical Model

Governing equation for fluid transport and gel mechanics

In this work, biphasic theory[10–19] has been employed to evaluate material physical parameters and to perform solute transport survey. A brief presentation of the field equations, as well as constitutive laws describing the system will be presented. Hereafter, we will adopt the following nomenclature: $\underline{u}$ and $\underline{v}$ are the solid displacement field and fluid phase velocity, ϕ^f is the fluid volume fraction, ϕ^s is the solid volume fraction, p is the fluid pressure, $\underline{\underline{\sigma}}$ is total stress tensor, $\underline{\underline{\sigma}}^e$ is the stress generated in the solid matrix; K [$m^4\ N^{-1}\ s^{-1}$] is the hydraulic conductivity, while Darcy's permeability, or intrinsic permeability will be denoted by the letter k [m^2]. The relationship between K and k is: $K = k/\eta$, where η [$N\ s\ m^{-2}$] is the fluid viscosity.

According to the biphasic theory, a polymer gel can be seen as an intimate mixing of a continuous solid and fluid phase. The momentum balance on the entire system is:

$$\underline{\nabla} \cdot \underline{\underline{\sigma}} = 0 \tag{1}$$

The total stress tensor $\underline{\underline{\sigma}}$ is composed by the stress in the solid and in the fluid phases, that under the assumption of phase incompressibility and irrotational fluid velocity field may be written as[14]:

$$\underline{\underline{\sigma}} = \underline{\underline{\sigma}}^e - p\underline{\underline{I}} \tag{2}$$

where $\underline{\underline{I}}$ is the identity tensor. The constitutive equation for the solid matrix assumed to behave as a hyperelastic solid, can be expressed in one-dimensional case for large deformation as[23,24]:

$$\sigma_z^e = \frac{1}{2} H_{A0} \left(\frac{\lambda^2 - 1}{\lambda^{2\beta+1}} \right) \exp\left[\beta\left(\lambda^2 - 1\right)\right] \tag{3}$$

where $\lambda(= 1 - \partial u/\partial z)$ is the stretch ratio along the load axis z (see Figure 1), H_{A0} is the aggregate equilibrium modulus at zero deformation ($\lambda = 1$) and β is a stiffening coefficient. Because of this special case of mono-dimensional geometry, all variables will vary along the coordinate z.[17] Therefore, the subscript "z" will be hereafter omitted.

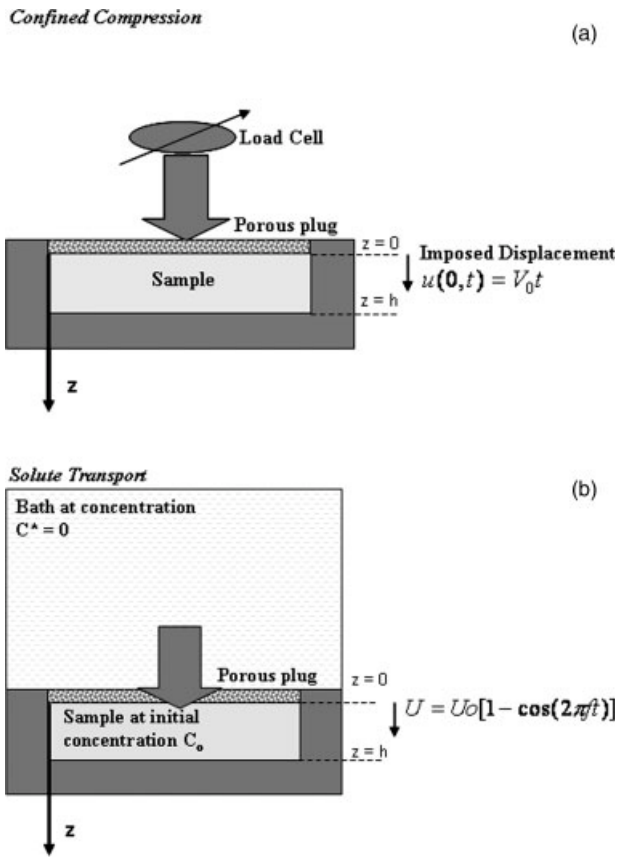

Figure 1. (a) Schematic representation of confined compression test; (b) geometry used in the transport simulations.

The continuity equation on the entire system, assuming intrinsic incompressibility for both solid and fluid phase, is[14]:

$$\underline{\nabla} \cdot \left(\phi^f \underline{v} + \phi^s \frac{\partial \underline{u}}{\partial t} \right) = 0 \tag{4}$$

For the specific case of confined compression geometry (Figure 1), the continuity equation becomes: $\phi^f v_z + \phi^s \frac{\partial u_z}{\partial t} = \text{const}$. The constant can be evaluated at $z = 0$, where $v^f = \frac{\partial u}{\partial t} = 0 \ \forall t$, so the relationship between fluid and solid velocity becomes

$$v^f = -\frac{\phi^s}{\phi^f} \frac{\partial u}{\partial t} \tag{5}$$

The friction generated during relative motion between the fluid and the solid phase is governed by the generalized Darcy's law:

$$\phi^f \left(\underline{v} - \frac{\partial \underline{u}}{\partial t} \right) = -\frac{k}{\eta} \underline{\nabla} p \tag{6}$$

where the permeability k was correlated to the deformation—in case of finite deformation—by the following equation[17]:

$$k = k_0 \left(\frac{\lambda - \phi_0^s}{1 - \phi_0^s} \right)^2 \exp\left[M \left(\lambda^2 - 1 \right) / 2 \right] \tag{7}$$

with the coefficient M that measures the sensitivity to the deformation, ϕ_0^s and k_0 are the solid volume fraction and Darcy's permeability at rest configuration respectively.

Governing equation for solute transport

To take in to account the solute transport in the gel, mass balance for the solute phase has to be considered as established by the following equation[13,14]:

$$\frac{\partial C}{\partial t} = -\underline{\nabla} \cdot \underline{J} \tag{8}$$

where, C is the average mass concentration of the solute in the gel, and $\underline{J}$ is the flux which is composed both by diffusive and connective term. The constitutive equation for the flux can be written as:

$$\underline{J} = \underbrace{-D_g \underline{\nabla} C}_{\text{Diffusion}} + \underbrace{C \chi \underline{v}}_{\text{Convection}} \tag{9}$$

where χ, named screening coefficient,[25] is a measure of the relative velocity between the solute and the fluid within the interstices and D_g ($=RD_0$) is the effective diffusion coefficient of the solute in the gel. To take into account the effect of deformation on R, the model proposed by Pluen et al.,[22] has been used:

$$\frac{D_g}{D_0} = \frac{1}{\left[1 + \frac{r_s}{\sqrt{k}} + \frac{1}{3} \left(\frac{r_s}{\sqrt{k}} \right)^2 \right]} \exp\left[-0.84 \left(\left(1 + \frac{r_s}{r_f} \right)^2 \phi^s \right)^{1.09} \right] \tag{10}$$

where, r_s is the Stokes radius for BSA set to 3.67 nm, r_f is the radius of agarose fibers set to 1.9 nm. The dependence of R by the deformation indirectly appears via k and ϕ^s.

Combining Eqs. 1, 5, and 6 the governing equation of gel elastodynamics can be written for the one-dimensional case as[17]:

$$\frac{\partial u}{\partial t} = \frac{k}{\eta \lambda} \frac{\partial \sigma^e}{\partial \lambda} \frac{\partial^2 u}{\partial z^2} \tag{11}$$

while combining the Eqs. 8 and 9, mass transport in the gel in the one-dimensional geometry (Figure 1b), is described by

$$\frac{\partial C}{\partial t} = D_0 \frac{\partial^2}{\partial z^2} (RC) + \chi \frac{\partial}{\partial z} (Cv) \tag{12}$$

The set of Eqs. 11 and 12, describes the coupling between molecular transport and deformation in a polymer gel in a mono-dimensional case.

Before proceeding with the definition of the boundary condition to solve the set of Eqs. 11 and 12, a discussion of the assumptions made in the above equations is necessary. In writing Eq. 12, we have not considered reversible binding that may occur between the polymer matrix and the solute. Binding may occur through electrostatic interaction between different chemical groups present on the solute and on the polymer, resulting in a molecular sticky effect. This may be seen as retardation both on the diffusive and convective transport occurring within the gel. Generally the presence of reversible binding on diffusion transport in polymers is modeled with a dual mobility approach.[26] The existence of two populations of the solute with two different mobility is postulated, namely the free and the bound species. The free and the bound species are related through a Langmuir-like adsorption isotherm that describes the binding of the solute molecule on the polymer backbone. By following this approach one recovers the same formal structure of the diffusion equation but the mutual diffusion coefficient is replaced by an apparent diffusion coefficient that takes into account the retardation because of binding.[27] The effect of the binding on convective transport can be included directly in the screening coefficient χ. Reversible binding between the solute and the polymer backbone will introduce a reduction of the parameter χ but the formalism of the equation will remain substantially unaltered. However, it has to be mentioned that since the binding phenomena is generally a saturable one, the effect of the binding brings about a strong concentration dependence both of apparent diffusion and screening coefficients at low concentration. Indeed, the binding will manifest its effect at concentration below the saturation threshold, while at higher concentration, when all the binding sites are saturated, the process is expected to occur as no binding was present.

The boundary conditions used in Eq. 11 to simulate periodic compression can be expressed as follows:

$$u(h,t) = 0, \ u(0,t) = U_0(1 - \cos(2\pi f t)), \ u(z,0) = 0 \tag{13}$$

where U_0 is the imposed displacement amplitude and it was set in order to give a deformation amplitude $\varepsilon_0 = 0.05$, 0.1, and 0.15, f is the loading frequency. The sample is considered being at rest in the initial configuration.

The study of macromolecular transport focused upon release kinetics in a gel where the initial solute concentration is C_o. The gel is assumed to be in contact with a porous plug

whose thickness is h_p. Porous plug allows fluid and mass transfer from the gel to the bathing solution at concentration C^* (Figure 1b). Boundary conditions for mass transport have been defined as follows:

$$\left.\frac{\partial C}{\partial z}\right|_{(h,t)} = 0, \quad C(0,t) = \varphi C_p^* \cong \varphi C^* \cong 0, \quad C(z,0) = C_o \quad (14)$$

where, φ is the partition factor depending on solid volume fraction of the gel[28] and C_p^* is the concentration at gel/plug interface. Nevertheless, solute concentration at the gel/fluid interface has been assumed as the gel was directly in contact with the bathing solution (C (0, t) $\cong$ φC^*). A detailed discussion on the assumptions made in writing the boundary conditions is also necessary. Boundary conditions (Eq. 14), are valid under the assumption that the mass transport resistance within the porous plug are negligible compared to that occurring in the gel and this implies that the plug has to have a high hydraulic conductivity (elevated porosity) and thickness much smaller than the gel. The mass transfer resistance posed by the porous plug depends upon its hydraulic conductivity, solute diffusivity and thickness. Because of the dimensionless form of the governing equations, the assumption that diffusive mass resistance in the plug is neglected is valid if the ratio between gel and plug thickness $\left(h_g/h_p\right)$ is much higher than one. The simulation has been carried out by assuming $h_g/h_p \geq 50$, where h_g is the gel thickness. Under these conditions, we can safely assume that the velocity field streamlines are continuous through the gel/plug interface (elevated hydraulic conductivity) and that concentration gradient and accumulation across the porous plug can be neglected (thickness ratio much higher than one). Furthermore, assuming both infinite dilution and ideal mixing in the bathing solution the external concentration has been set equal to zero ($C^* \cong 0$). It has also to be mentioned that the conditions of elevated stiffness of the porous plug is necessary in order to write Eq. 11. Indeed, if the porous plug was compliant, than its deformation should be taken into account in order to evaluate the displacement of the gel at the plug interface.

Furthermore, in Eq. 12, the screening coefficient (χ) was set to unity. According to Jhonston and Deen,[25] this factor depends upon the hydrodynamic radius of the solute, its charge as well as the properties of the gel, and may assume values either greater or smaller than unity.[14] Moreover, in order to take in to account the reduction of the diffusivity ratio with the deformation, R has been kept constant at strain offset $\varepsilon_0/2$.

Following the approach proposed by Mauck et al.,[15] the set of Eqs. 11 and 12 and their boundary conditions (Eqs. 13 and 14) were rewritten in term of the following dimensionless variables:

$$\hat{z} = \tfrac{z}{L}, \quad \hat{u} = \tfrac{u}{L}, \quad \hat{t} = \tfrac{D}{L^2}t, \quad \hat{c} = \tfrac{C}{C_0}, \quad \hat{f} = \tfrac{L^2}{kH}f \qquad (15)$$

and the resulting equations discretized in the space domain and arranged in a set of ODEs.

Experimental

Gel preparation

Agarose gels with concentrations of 2, 4, and 6% (w/v), respectively, were prepared by dissolving agarose powder type VII (Sigma) in PBS 0.01M at 80°C. After complete solubilization the solution was cast in a stainless mould in order to get cylindrical disks of 10 mm in diameter and 1 mm in thickness and keep at 4°C to allow gelling. In the following sections, it will be referred to agarose 2, 4, and 6% as gel2, gel4 and gel6, respectively.

Mechanical testing

The plugs were tested with a Dynastat mechanical spectrometer (IMASS Inc) operated at displacement control (stress-relaxation mode). The mechanical apparatus was interfaced with a computer by DAQ PCI-MIO 16XE NATIONAL INSTRUMENTS and controlled by LABWIEV® National Instruments. Each plug was placed inside a smooth confining cylindrical polycarbonate chamber. The top surface of the specimen was loaded in compression through a porous filter. Prior to the actual tests a preconditioning compression of 5% was applied on the construct in order to allow the correct positioning of the specimen in the chamber. In the following stress-relaxation test, the specimen was displaced by a sequence of compression ramps each with a duration of the period t_0 = 60 s at a rate of V_0 = 1.6 μm s^{-1}. Each ramp induced a 5% strain followed by a relaxation phase of $\sim$ 1000s. Load evolution was registered by a load cell and the stress was evaluated by dividing the load value over the cross section (Figure 1a). Furthermore, from the values of the plateau stress the corresponding stress strain equilibrium curve was obtained (Figure 2a).

Darcy's permeability and aggregate modulus evaluation

The mechanical and fluid transport parameters evaluation has been carried out by curve fitting experimental stress relaxation curve by solving the Eq. 11. The prescribed boundary conditions to Eq. 11 have been set as follows:

$$u(0,t) = \begin{cases} V_0 t \rightarrow 0 \leq t \leq t_0 \\ V_0 t_0 \rightarrow t_0 \leq t \end{cases}, \quad u(h,t) = 0, \quad u(z,0) = 0 \qquad (16)$$

The procedure used to evaluate the parameters H_{A0}, β, k_0, and M has been carried out in a similar fashion to that developed by Ateshian et al.,[17] and Iatridis et al.,[18] for cartilaginous tissue and used elsewhere[19] for agarose-chondrocytes constructs. Equation 3 has been employed to evaluate the parameters H_{A0} and β, via curve fitting equilibrium stress strain curve shown in Figure 2b. Then, the theoretical stress at interface $\sigma^e(\partial u/\partial z)|_{z=0}$ has been employed to fit the experimental stress relaxation curve with k_0 and M as fitting parameters.

Diffusion coefficient measurements

For the diffusion measurements cylindrical samples of agarose (2%, 4%, 6% w/v) were incubated for 18 h in a medium containing 0.02 mg/ml of 68-kDa bovine serum albumin (BSA) fluorescein isothiocyanate (FITC)-conjugated (Molecular Probe).

Diffusion coefficients of the probe were measured by the fluorescence recovery after photobleaching (FRAP) technique. The in-house-made apparatus is composed of an upright microscope (AX60 Olympus), a mercury lamp (100 W; USH-02D Ushio) equipped with a shutter, an argon

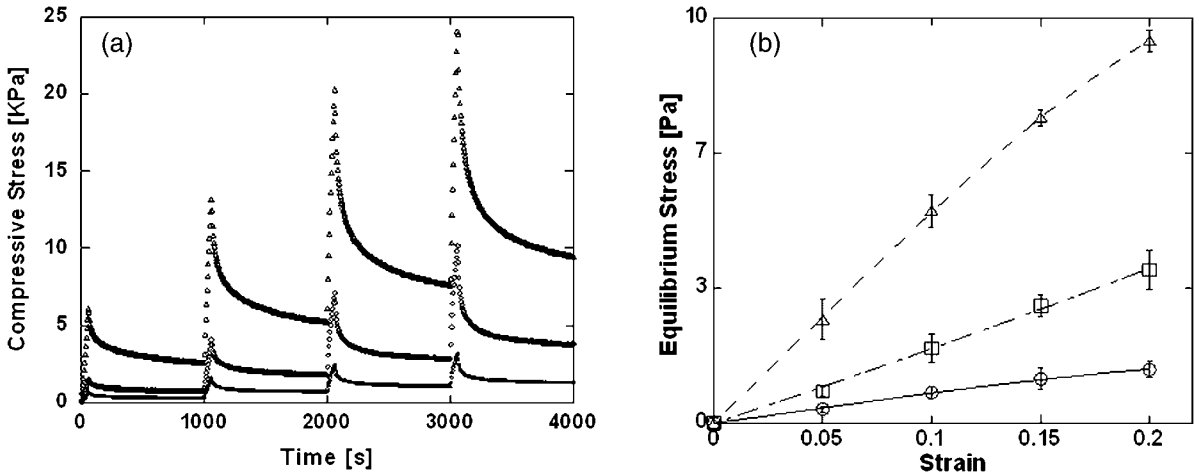

Figure 2. Mechanical test performed on agarose gels at 2% (○), 4% (□), and 6% (△) (w/v).

Stress relaxation tests (a). Equilibrium stress–strain curves (b) Data show an increase in mechanical properties with gel concentrations.

laser (488 nm; Innova 90-2) with shutters, a spatial filter (100 mm; M900 Newport) aligned with the microscope optical path, a charge-coupled device (CCD) camera (PENTAMAX, Princeton Instruments), and a personal computer (PC) to store and analyze the images acquired. A selected region of the fluorescent sample was exposed briefly to intense monochromatic laser light, causing local photobleaching. The process of fluorescence redistribution was recorded in a series of digital images and then processed. The diffusion coefficient was evaluated via spatial frequency analysis (SFA) as described elsewhere.[19,20] The time synchronization between laser shutter, camera shutter, camera, and Hg lamp was controlled through Metamorph journals (Metamorph, Image Analysis Software) and the images were analyzed via a specifically developed Matlab® (MathWorks) program. FRAP experiments were repeated five times for each sample and for free solution. In this manner, the ratio between effective diffusivity in the gel and diffusivity in solution (D_g/D_0) was determined.

Results

Darcy's permeability and aggregate modulus

The first step of this work has been the evaluation of nonlinearity of the system in terms of Darcy's permeability, elastic modulus and molecular diffusivity in different agarose gels. Stress relaxation tests indicated that the mechanical strength of agarose gels increased with gel concentrations (Figure 2a). This is also confirmed by the equilibrium stress–strain curve illustrated in Figure 2b, where mechanical stiffness of agarose gels increased with gel concentration. For up to 15% of strain no significant variation with deformation was detected; stiffening parameter β in Eq. 3 was close to zero and did not show any particular variation trend with agarose concentration.

At deformation values greater than 15%, a decrease of mechanical modulus was observed. This effect was probably due to plasticization phenomena or to a different type of nonlinear elasticity; both factors were not taken into account in the network constitutive equation (Eq. 3). The curve fitted value for H_{A0} increased with gel concentration showing a trend that is in agreement with previous literature reports[29]—data are shown in Table 1. In Figure 3, Darcy's permeability correlation with strain at each gel concentration was obtained by plotting Eq. 7 with the values of K_0 and M obtained by curve fitting the raw data acquired during the stress relaxation tests. The initial solid fraction ϕ_0^s value was evaluated as previously reported by Pluen et al.,[22] and Johnsonn and Deen.[30] The Darcy's permeability at zero strain k_0, decreased with agarose concentration as reported also by Johnsonn and Deen.[30] Coefficient M did not show any specific trend of variance with agarose concentration: 2.36 ± 0.89 at 2% (w/v), 2.85 ± 2.10 at 4% (w/v) and 1.75 ± 0.98 at 6% (w/v) (see Table 1).

However previously reported measurements of Darcy's permeability were carried out in small deformation range and the strain dependent relationship was generated by introducing the dependence of porosity with deformation.[29] This may explain the minor differences between the results of the latter survey and our work; these, in turn, may also be due to the

Table 1. Physical Values of Agarose Gels in Table are Reported Elastic Equilibrium Modulus at Zero Strain (H_{A0}), Intrinsic Hydraulic Permeability (k_0), Strain Dependent Hydraulic Permeability Coefficient (M) as Mean ± s.d With $n = 3$, Obtained by Curve Fitting Stress Relaxation; Diffusivity Ratio Data ($R = D_g/D_0$) as Mean ± s.d With $n = 5$ Obtained by FRAP and Values of ϕ_0^s Obtained by Ref. 28

Gel (% w/v)	ϕ_0^s [Ref. 28]	k_D [nm^2][Ref. 30]	H_{A0} [KPa]	K_0 [nm^2]	M	D/D_0
2	0.0190	616	7.2 ± 3.1	660.4 ± 90.96	2.36 ± 0.89	0.81 ± 0.07
4	0.0390	132	17.6 ± 2.5	133.5 ± 44.18	2.85 ± 2.10	0.53 ± 0.02
6	0.0585	33	51.8 ± 5.8	43.0 ± 18.30	1.75 ± 0.98	0.41 ± 0.05

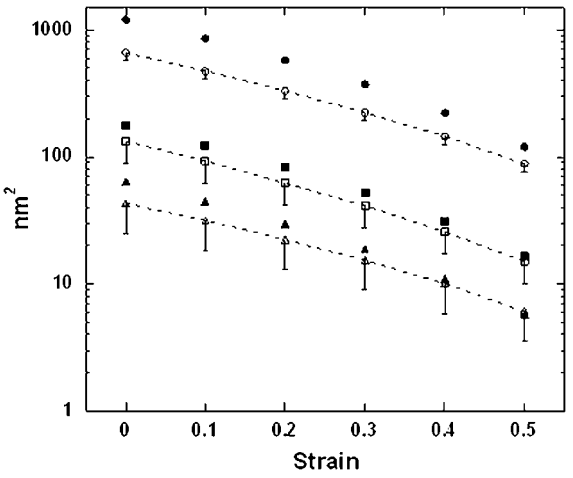

Figure 3. Darcy's permeability vs. strain for agarose 2% (○, ●), 4% (□, ■), and 6% (△, ▲) (w/v).

Empty markers refer to data obtained in this work. The curves are obtained by plotting Eq. 7 with data reported in Table 1. Data labelled by full markers refer to strain dependent permeability obtained by Gu et al.[29]

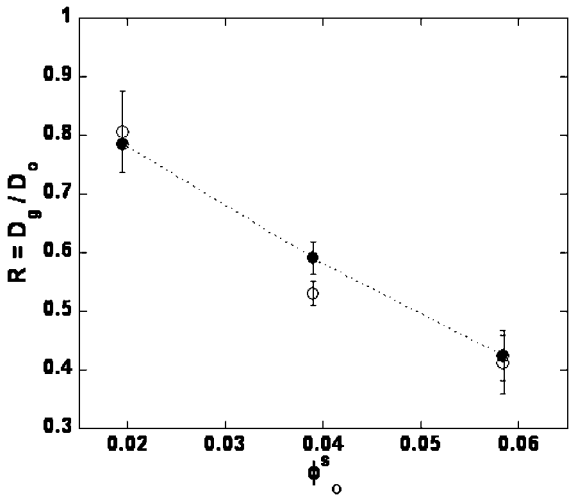

Figure 4. Diffusivity ratio ($R = D_g/D_o$) of BSA in agarose gel at different gel concentration.

Empty markers are experimental data obtained with FRAP and full markers/dotted line is the prevision of diffusivity ratio by using Eq. 10.

approximation in evaluating the deformation field in the sample by using a linear biphasic model.

Furthermore, it has also to be mentioned that the conditions of elevated hydraulic conductivity along with high stiffness of the porous plug are necessary in order to assure that the presence of the porous plug can be neglected to analyze the mechanical data and hydraulic conductivity data. Indeed, if the hydraulic conductivity of the porous plug would be comparable or less than the hydraulic conductivity of the agarose gel, than the mechanical data would be affected by the hydrostatic pressure gradient across the porous plug. We have verified, before carrying the mechanical experiment, that the hydraulic conductivity of the porous plug was several order of magnitude higher than the hydraulic conductivity of the agarose gel.

Diffusivity ratio

The values of diffusivity ratio in the free swelling state decreased as gel concentration increased. The values of R against ϕ_0^s for FITC-BSA are shown in Figure 4 by empty circles. In order to take into account the effect of deformation on molecular diffusivity, a modified Brinkman equation's has been used (Eq. 10). This equation has been evaluated using Darcy's permeability and solid volume fraction values at zero strain. As shown in Figure 4 (full circles/dotted line), the predicted values of R at zero strain were in good agreement with the experimental values of R at zero strain (Figure 4, empty circle). Consequently, Eq. 10 has been used to obtain the values of diffusivity at each level of deformation by means of the relationship between hydraulic conductivity and deformation (Eq. 7). As shown in Table 2, the diffusivity ratio R decreases by increasing deformation at each agarose concentration.

Simulation of solute release

The physical parameters H_{A0}, β, K_0, M, and R obtained experimentally, were used to simulate the solute transport and release from agarose gel under cyclical loading. Simulation have been carried out by solving the dimensionless form of Eqs. 11 and 12, with boundary conditions expressed in Eqs. 13 and 14, using the physical parameters reported in Tables 1 and 2. Sample thickness hg was set to 0.001 m; displacement loading frequency varied within the range from 0.001 to 1 Hz. The values of diffusivity used in Eq. 12 at each level of strain amplitude are reported in Table 2.

All simulations were performed up to a computational time of 15,000 s. In Figure 5a is reported the concentration profile (C/C_0) within the gel at final computation time. Boundary conditions are respected, with zero concentration at interface ($z/h = 0$) and no flux at bottom ($z/h = 1$). The distortion in the profile induced by mechanical stimulation is evident. In Figure 5b the rates of mass released from gel are illustrated as the ratio M_t/M_0. M_t is the bioactive agent mass in the gel at time t, calculated by integrating the concentration profiles along sample thickness over time, and M_0 is the mass at time zero, respectively.

As shown in Figure 5b the rate of macromolecular mass release was found in general to increase with loading frequency. At low frequency and amplitude, no significant differences between diffusive ($f = 0$ Hz) and mechanical activated transport ($f > 0$ Hz) were recorded. By increasing the loading frequency and amplitude, the mass transfer is accelerated through the gel.

Table 2. Diffusivity Values Used in the Simulation

	$R = D_g/D_o$		
Gel (%)	$\varepsilon/2 = 0.025$	$\varepsilon/2 = 0.05$	$\varepsilon/2 = 0.075$
2	0.797	0.777	0.768
4	0.577	0.562	0.547
6	0.415	0.397	0.383

Data were obtained by coupling Eqs. 7 and 10. Reported data refer to strain amplitude $\varepsilon_0/2$ (=0.025, 0.05, and 0.075).

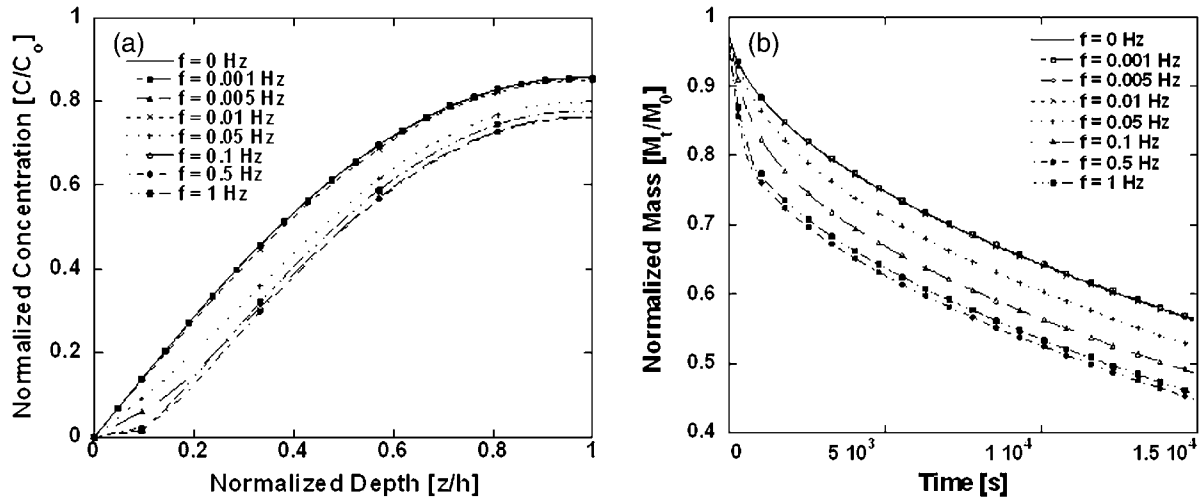

Figure 5. Numerical results.

Concentration in the sample at 15,000 s with frequency (a). Mass release kinetics up to 15,000 s at different frequencies (b). Simple diffusion case correspond to f = 0 Hz. The surface is located at normalized depth z/hg = 0.

To evaluate the differences in mass released at final computational time, the mass release gain (G) has been introduced:

$$G = 100|(m_{\text{conv}} - m_{\text{diff}})/m_{\text{diff}}|_{t=15{,}000\ \text{s}} \tag{17}$$

where m_{conv} is the mass released by convection/diffusion and m_{diff} is the mass released by simple diffusion. The results graphically illustrated in Figure 6, show the variance of G for gel2 as a function of frequency, at three different strain amplitudes (ε = 0.05, 0.10, 0.15). More specific, at 5% of strain amplitude (Figure 6, solid line) G monotonically increases with frequency. Higher G values were obtained by increasing strain amplitude. At strain amplitude of 15%, G reached a maximum with frequency. In Figure 6—dotted-line—are also shown the predicted values of G for agarose gel6, at 15% of strain amplitude; the gain for gel6 behaves in a similar fashion. A slight increase of G values when compared to gel2 was observed. Along these lines, G variance curve for gel4 had a similar sigmoid-shape (data not shown) to the ones already drawn for agarose gel2 and gel6, respectively.

Data reported in Figures 5 and 6, indicate that the kinetics of solute transport depend upon load parameters, frequency and amplitude, as well as of physical parameters K, H, and D.

To investigate the synergistic effect of material and loading parameters on the mechanical/transport behavior of the system, simulations have been carried out by varying dimensionless parameters describing the elastodynamics of the biphasic systems[15]:

$$R_g = \frac{KH}{RD_o};\ \hat{f} = \frac{h^2}{KH}f;\ Pe = \varepsilon_0 \hat{f} R_g \tag{18}$$

where R_g represents the ratio between the characteristic diffusive time of solute in the gel $Td = h^2/RD_0$ to the percolation time $Tp = h^2/KH$; $\hat{f}$ represents the ratio between percolation time to period of the solicitation and P_e is the Peclet number of the system. It is important to note that the dimensionless frequency corresponds to the Deborah's number of the system, D_e.[31]

The curves illustrated in Figure 6 were analyzed in the light of above mentioned dimensionless parameters. In Figures 7 and 8, are shown the predicted values of gain obtained by varying the dimensionless parameters. As shown in Figure 7, by keeping the strain amplitude constant at 0.05, while increasing R_g from 10 (Figure 7 solid line) to 1000 (Figure 7 dotted line), the gain was also increased. Moreover, the effect of strain amplitude was investigated, as shown in Figure 8; in particular, at constant R_g = 10, by increasing the strain amplitude from 5% (ε = 0.05, Figure 8 solid line) to 20% (ε = 0.20, Figure 8 dotted line) the gain was increased.

Results shown in Figure 7 indicate that the gain values are more affected by R_g than by strain amplitude. The deformation affects primarily the inflection point of the curves, as well as the maximum of the G curves.

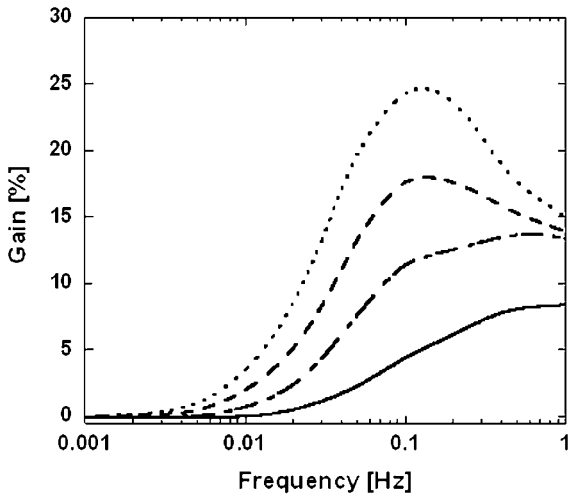

Figure 6. Gain in mass released with frequency.

Data correspond to prevision on G for agarose 2% at ε = 0.05 (continuous line), ε = 0.10 (dot-dashed line), ε = 0.15 (dashed line). In figure is also reported data relative to agarose 6% at ε = 0.15 (dot-line).

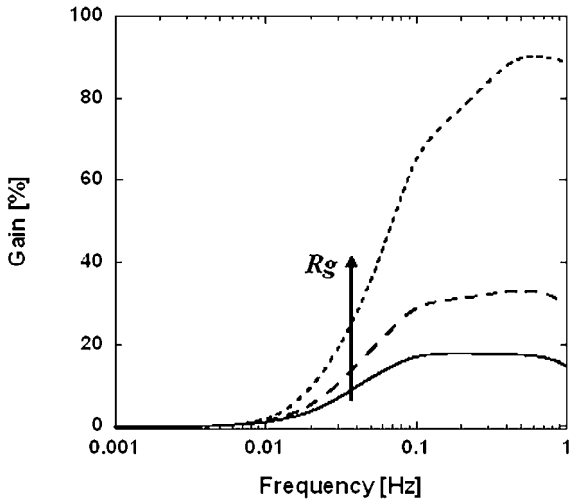

Figure 7. Influence of R_g on gain.

The curves were obtained at constant deformation (ε = 0.05), and by varying R_g. R_g = 10 (solid line), 100 (dashed line), 1000 (dot line).

Discussion

The aim of this work was to study the effect of mechanical loading on solute transport in soft gels used as matrices in drug delivery systems and tissue engineering applications. As material model agarose gel has been used, while nonlinear biphasic theory was employed to characterize the material and to simulate solute distribution within it.

The material properties that regulate mechanical, fluid, and solute transport in soft gels are hydraulic conductivity, aggregate modulus, and macromolecular diffusivity.[15] Since large deformation has been taken into account, it was necessary to evaluate both hydraulic conductivity and aggregate modulus vs. deformation relationships. Furthermore, the influence of deformation upon the diffusion coefficient has been quantified as well. Measurements of solute diffusivity in agarose gel at zero strain have been performed by using FRAP technique. With the apparatus employed for our purposes, it was not possible to evaluate the relationship between diffusion coefficient and deformation. To overcome this limitation and to recover the dependence of diffusivity by deformation, the experimental Darcy's permeability was introduced in the modified Brinkman's equation (Eq. 10).

Simulation of solute transport within polymeric gels for large deformation, suggested interesting dependence trends of release profile upon frequency. Simulations have been carried out by using physical material parameters, named Darcy's permeability (k), elastic modulus (H_A), and macromolecular diffusivity (D_g), experimentally evaluated on agarose gels. Therefore, the simulated results should be regarded as a numerical prediction. A similar approach has been recently used by Mauck el al.[15] and Sengers et al.,[16] although it was assumed physical material properties not dependent on deformation, and their values were lent by literature. Furthermore, the solute transport has been investigated both under static condition and dynamic loading. The influence of dynamic load on equilibrium partition factors at steady state has been reported. In this work, our attention has been focused upon the evolution of the release kinetics, and in particular, how mechanical deformation, frequency and materials properties affect the transport mechanism.

The solute concentration profile within the gel at final computation time (Figure 5a) was evidently different in the presence of mechanical stimulation, when compared to simple diffusion (f = 0 Hz). Furthermore, as shown in Figure 5a, the concentration at each material coordinate in the loaded case, was lower than the concentration in the unloaded case and therefore faster mass release from the gel (Figure 5b). In order to define the influence of material properties and loading conditions (frequency and deformation) on mass transport, the gain function (G) has been featured (Eq. 17). In Figure 6, the gain (G) for the gels calculated for different frequency values are reported and parametrized as a function of loading amplitude. The function G is sigmoid-shaped, showing values close to zero at low frequency followed by a sharp transition where G increased rapidly reaching a plateau at higher frequencies. The shape of the curves changes depending upon deformation amplitude and gel composition. Although all the curves present a similar sharp change of curvature, with the onset of the curvature change at a cut-off frequency (f_c) some of them also present a maximum at a given frequency (f_{max}). The change of curvature indicates a transition between a diffusion controlled transport region ($f < f_c$) to a convection enhanced transport region ($f > f_c$). In some cases, a maximum in G is observed due to a positive combination of mechanical stimulus and material parameters that maximise the enhancement in mass transport due to convection. It can be seen that for different curves, f_c, f_{max}, and G_{max}, depend upon gel composition and loading parameters. Therefore, their behavior can be further investigated in the light of the governing dimensionless parameters (Eq. 18). At constant deformation, the curves are "iso-R_g", and, therefore, the competition between percolation and diffusion is governed by the loading parameters; concomitantly, by increasing the frequency D_e and P_e also increase.

On the other hand, at constant frequency by increasing the deformation, R_g, D_e, and P_e vary, and the trend of variance

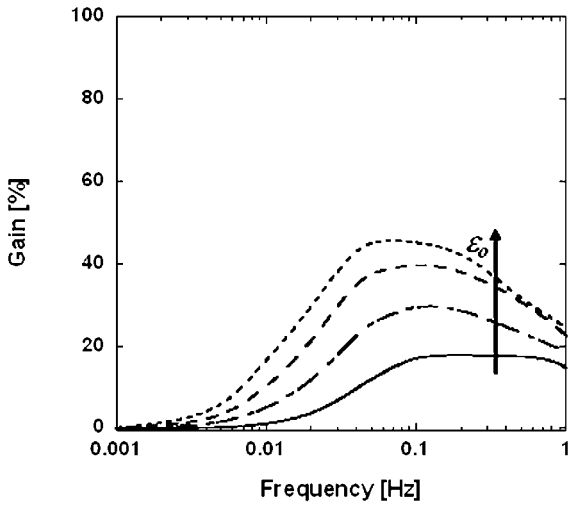

Figure 8. Effect of deformation on gain.

The curves were obtained at constant R_g = 10, and by varying strain amplitude; ε = 0.05 (solid line), 0.10 (dot-dashed line), 0.15 (dashed line), 0.20 (dotted line).

depends on the interdependence of physical parameters and deformation. The slight increase of G_{max}, observed in the gel6 at $\varepsilon = 0.15$ when compared to that of gel2, can be interpreted as the result of P_e variation. Indeed, R_g decreases from 90 to 35 for gel2 and gel6, respectively. G_{max} is expected to decrease by decreasing R_g (Figure 7); this result clearly demonstrates that R_g is not the unique parameter that affects G_{max}. At $\varepsilon = 0.15$, P_e for gel6 is about double of that for gel2, contributing further on convective transport.

Moreover, as shown in Figure 6 a transition occurs between the two transport mechanisms in a frequency dependent manner. The cut-off frequency (f_c) is the parameter that defines the switch over. At frequencies below the f_c, the principal release mechanism from the gel is simple diffusion. In this frequency range, the gain is low and the kinetics of transport mechanism is mainly governed by D_g. This becomes also evident in Figure 5, where the normalized mass release variance plots at low frequencies fit well to kinetic profiles governed by diffusion kinetics (Figure 5, $f = 0$ Hz).

Gain sharply increases for load frequency values higher than f_c, indicating that convection is taking place, and, therefore, not only there is an enhancement in gain, but also a change of the release kinetics. Indeed, in Figure 5, at higher frequency the profile of mass released is different by diffusion kinetics.

The cut-off frequency depends mainly upon strain amplitude and less on material properties. As shown in Figure 7, by increasing R_g by three orders of magnitude the cut-off frequency f_c remained unchanged, but G_{max} increases. In Figure 8 the effects of strain amplitude on the gain curve are reported. At constant R_g, the strain amplitude increase lowered the cut frequency f_c. In this case G_{max} is also affected, but the variation is more flat compared to Figure 7.

By analyzing the curves reported in Figures 6–8 it was shown that after the inflection point the gain can reach a plateau or a maximum value as a function of frequency. This, in turn, has been tentatively interpreted as the effect of Deborah's number on fluid velocity field. In general, Deborah's number strongly affects the mechanics of polymer gels[31]; in the case of biphasic systems, it influences also the fluid velocity. As depicted in Figure 9, at high Deborah's number values, a high velocity field is confined in the region close to the surface of the system while the fluid velocity is close to zero in the deeper region. At low Deborah's number, the velocity field is more homogeneously distributed, but the intensity is lower.

Therefore, at high D_e only the layers close to the surface are able to transfer mass from the gel, even though at a higher velocity the amount of solute released is decreased. This could lead to saturation phenomena (or inversion in some cases) observed for G at higher frequency and strain amplitudes. The predictions on the kinetics of solute transport, presented in Figures 5–8, give important hints for optimizing a delivery protocol. Once determined the physical properties of the gel and the bioactive agents, in terms of elastic moduli and hydraulic conductivity and macromolecular diffusivity, the dimensionless parameters are known. Therefore, it is possible to determine one or more optimal load frequencies which fulfil the requirements in terms of delivery time and kinetic release.

The model presented herein, reveals interesting features of the coupled macromolecular transport under periodic mechanical stimuli. In spite of assumptions, the formulation does describe in a satisfactory manner the influence of dynamic mechanical stimuli on coupled elastodynamics and fluid transport mechanisms in macromolecular biphasic systems in the field of large deformations.

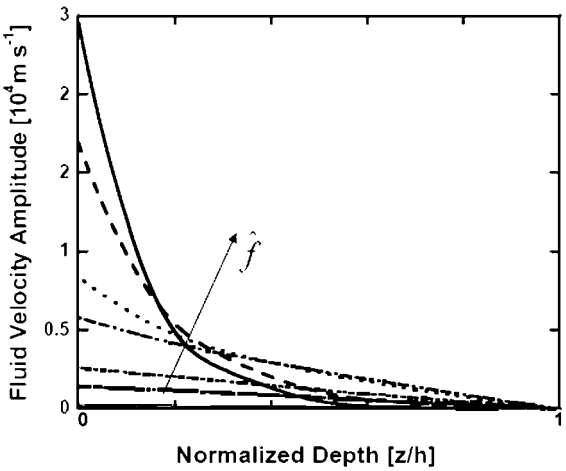

Figure 9. Effect of *De* on fluid velocity filed reported as fluid velocity amplitude vs. gel depth parametric in $\hat{f}$.

Fluid velocity increase with Deborah's number. The effect is evident mainly in the region close to the surface ($z/h = 0$).

Implication for Drug Delivery

The model prediction will be further exploited to formulate novel approaches that will help in enhancing and controlling macromolecular distribution within soft hydrated tissues to optimize drug delivery protocols to be used in therapy and diagnostics. These approaches include direct flow infusion protocols that may be improved by oscillating infusion pressure or flow as well as by defining periodic mechanical deformation of the tissue.

Indeed, the present study provides the means to improve the design of drug delivery systems based on polymeric matrices. Polymeric hydrogels have been largely used as bioactive agents delivery systems.[1–3] Generally, these devices are engineered to operate under mechanically static conditions. In vitro studies have shown that under dynamic loading conditions, solute transport in polymeric matrices (i.e., tissue explants or hydrogels) is affected by mechanical load.[8,14,32] Furthermore, in vivo studies have proven that mechanical stimuli are able to guide the release of bioactive agents[9] and to promote and modulate tissue regenerations.[32,33] By adopting the approach proposed in this work and by others,[15] namely understanding the fundamentals of the coupling between mechanical stress and deformation and mass transport in gels will render plausible the design of "smart" drug delivery systems, actively bio-responsive and triggered by biological mechanical stress. The results reported in Figure 6–8, clearly show that bioactive agent release profiles may be properly tuned and modulated, for a given mechanical environment by an accurate choice of material properties. Indeed, it is possible to tune the release activation on mechanical stimuli, such as frequency and strain amplitude, and at the

same time, control the release kinetics of virtually, any biological agent through the material properties such as elastic moduli and hydraulic conductivity of the gel.

The effect of mechanical stimuli on the release of bioactive agents depends upon physiochemical properties of the polymer matrix and the diffusing drug as well as on their interaction. Therefore to design polymer gel matrices that may take advantage of controlling release profile of bioactive drug in upon the biomechanical dynamic environment the effect of the main drug parameters that control the transport process should be discussed. In particular the drug molecular weight and its charge may have profound effect on the mechanism of delivery. In general, convection enhanced transport is more effective on high molecular weigh molecules and therefore better performance of mechanically-activated drug delivery platforms should be expected for large therapeutics. The switching behaviour showed in Figure 7, is more likely to be observed for large therapeutics than for small molecular weight drugs, although this depend upon the ratio between the solute and polymer gel mesh sizes. This is corroborated by experimental evidence that mechanical activated delivery from polymer gels is very effective for large molecular weight growth factors such as VEGF.[9] Drug charge may effect the extension of reversible binding between the drug molecule and the polymer network influencing both diffusion and convection transport. Highly charged molecule may interact strongly with the polymer network leading to a strong retardation, or apparent hindrance, to transport and therefore reduce the effect of convection enhanced delivery. However, this effect is expected to be more evident at low concentration while it is supposed to vanish at high drug concentration when all the binding sites of the polymer network are saturated.

The survey presented here, which couples the mechanical deformation with the transport of macromolecules within a polymer gel, is a tool in the service of engineering polymer matrices with a fine control of release profiles depending upon the preset mechanical environment. Furthermore, our macromolecular transport simulation model will serve to optimise the techniques for enhancing drug loading efficiency in polymer gels. Eventually, our model will find application also in bioreactor design and tissue engineering[34,35] as its adoption will make possible the optimisation of load history, gel scaffold properties and bioactive agents transport mechanism modulation, in concert with cell requirements and to tune ultimately tissue growth and biosynthesis.

Conclusion

Biphasic theory has been adopted and used to describe the coupling between mass transport and gel mechanics in the large deformation range. The model indicates that by tuning the material parameters it is possible to design platforms able to actuate and control release kinetics. Of particular interest the frequency switch predicted for these materials that may deserve further experimental validations.

Literature Cited

1. Shea LD, Smiley E, Bonadio J, Mooney DJ. DNA delivery from polymeric matrices for tissue engineering. *Nat Biotechnol.* 1999;17: 551–554.
2. Baldwin SP, Saltzman WM. Materials for protein delivery in tissue engineering. *Adv Drug Deliv Rev.* 1998;33:71–86.
3. Jen AC, Wake MC, Mikos AG. Review: hydrogel for cell immobilization. *Biotechnol Bioeng.* 1996;50:357–364.
4. Quinn TM, Kocian P, Meister JJ. Static compression is associated with decreased diffusivity of dextrans in cartilage explants. *Arch Biochem Biophys.* 2000;384:327–334.
5. Garcia AM, Frank EH, Grimshaw PE, Grodzinsky AJ. Contributions of fluid convection and electrical migration to transport in cartilage: relevance to loading. *Arch Biochem Biophys*, 1996;333:317–325.
6. O'Hara BP, Urban J, Maroudas A. Influence of cyclic loading on the nutrition of articular cartilage. *Ann Rheum Dis.* 1990;49:536–539.
7. Maroudas A. Biophysical chemistry of cartilaginous tissues with special reference to solute and fluid transport. *Biorheology.* 1975;12:233–248.
8. Evans RC, Quinn TM. Dynamic compression augments interstitial transport of a glucose-like solute in articular cartilage. *Biophys J.* 2006;91:1541–1547.
9. Lee KY, Peters MC, Anderson KW, Mooney DJ. Controlled growth factor release from synthetic extracellular matrices. *Nature.* 2000; 408:998–1000.
10. Mow VC, Kuei SC, Lai WM, Armstrong CG. Biphasic creep and stress relaxation of articular cartilage in compression. theory and experiments. *J Biomech Eng.* 1980;102:73–84.
11. Levenston ME, Frank EH, Grodzinsky AJ. Variationally derived 3-field finite element formulations for quasistatic poroelastic analysis of hydrated biological tissues. *Comput Methods Appl Mech Eng.* 1998;156:231–246.
12. Huyghe JM, Janssen JD. Quadriphasic mechanics of swelling incompressible porous media. *Int J Eng Sci.* 1997;35:793–802.
13. Netti PA, Baxter LT, Boucher Y, Skalak R, Jain RK. Macroscopic and microscopic fluid transport in living tissues—application to solid tumors. *AIChE J.* 1997;43:818–834.
14. Netti PA, Travascio F, Jain RK. Coupled macromolecular transport and gel mechanics: poroviscoelastic approach. *AIChE J.* 2003;49:1580–1596.
15. Mauck RL, Hung CT, Ateshian GA. Modelling of neutral solute transport in a dynamically loaded porous permeable gel: implications for articular cartilage biosynthesis and tissue engineering. *J Biomech. Eng.* 2003;125:602–614.
16. Sengers BG, Oomens CWJ, Baaijens FPT. An integrated finite-element approach to mechanics, transport and biosynthesis in tissue engineering. *J Biomech Eng.* 2004;126:82–91.
17. Ateshian GA, Warden WH, Kim JJ, Grelsamer RP, Mow VC. Finite deformation biphasic material properties of bovine articular cartilage from confined compression experiment. *J Biomech* 1997;30:1157–1164.
18. Iatridis JC, Setton LA, Foster RJ, Rawlins BA, Weidenbaum M, Mow VC. Degeneration affects the anisotropic and nonlinear behaviours of human annulus fibrous in compression. *J Biomech.* 1998;31: 535–544.
19. Derosa E, Urciuolo F, Borselli C, Gerbasio D, Imparato G, Netti PA. Time and space evolution of transport properties in agarose–chondrocyte constructs. *Tissue Eng.* 2006;12:2193–2201.
20. Berk DA, Yuan F, Leunig M, Jain RK. Fluorescence photobleaching with spatial Fourier analysis: measurement of diffusion in light scattering media. *Biophys J.* 1993;65:2428–2436.
21. Gu WY, Yao H, Vega AL, Flagler D. Diffusivity of ions in agarose gels and intervertebral disc: effect of porosity. *Annl Biomed Eng.* 2004;32:1710–1717.
22. Pluen A, Netti PA, Jain RK, Berk DA. Diffusion of macromolecules in agarose gels: comparison of linear and globular configurations. *Biophys J.* 1999;7:542–552.
23. Cohen B. *Anisotropic hydrated soft tissues in finite deformation. Ph.D. Thesis*, Columbia University, New York, 1992.
24. Cohen B, Lai WM, Mow VCJ. A transversely isotropic biphasic model for unconfined compression of growth plate and chondroepiphysis. *J Biomech Eng ASME.* 1998;120:491–496.
25. Johnston ST, Deen WM. Hindered convection of proteins in agarose gel. *J Membr Sci.* 1999;42,5.
26. Koros WJ. Model for sorption of mixed gases in glassy polymers. *J Polym Sci Phys Ed.* 1980;18:981.
27. Astarita G. *Mass transfer with chemical reaction.* Elsevier, Amsterdam, 1967.
28. Lazzara MJ, Deen WM. Effects of concentration on the partitioning of macromolecule mixtures in agarose gels. *J Colloid Interface Sci.* 2004:272:288–297.

29. Gu WY, Yao H, Huang CY, Cheung HS. New insight into deformation-dependent hydraulic permeability of gels and cartilage. *J Biomech*. 2003;36:593–598.
30. Johnson EM, Deen WM. Hydraulic permeability of agarose gels. *AIChE J*. 1996;42:1220–1224.
31. Macosko, CV. *Rheology: Principles, Measurements, and Applications*. NJ: Wiley, 1994.
32. Sah RL, Kim YJ, Doong JY, Grodzinsky AJ, Plaas AH, Sandy JD. Biosynthetic rensponse of cartilage explants in response to dynamic compression. *J Orth Res*. 1989;7:619–636.
33. Niklason LE, Gao J, Abbot WM, Hirschi KK, Houser S, Martini R, Langer R. Functional arteries growth in vitro. *Science*. 1999;284:489–493.
34. Kim BS, Nikolovsky J, Bonadio J, Mooney DJ. Cyclic mechanical strain regulates the development of engineered smooth muscle tissue. *Nat Biotechnol*. 1999;17:979–983.
35. Chowdhury TT, Bader DL, Shelton JC, Lee DA. Temporal regulation of chondrocyte metabolism in agarose constructs subjected to dynamic compression. *Arch Biochem Biophy*. 2003;417:105–111.

Manuscript received Jun. 7, 2007, and revision received Nov. 7, 2007.